

---

## Attenuation Correction Procedures

---

*Jack L. Parker*

### 6.1 INTRODUCTION

The nondestructive assay (NDA) of nuclear material must deal with large sample sizes and high self-absorption. Typical containers range from 2-L bottles to 220-L drums, and even a small sample with a high concentration of nuclear material has significant self-attenuation. Although gamma-ray self-attenuation may frequently be ignored in the filter papers or small vials encountered in radiochemical applications, it usually cannot be ignored in NDA measurements of nuclear material.

Because the size and shape of nuclear material samples vary widely, it is difficult to construct appropriate calibration standards. In principle, calibration standards are not needed if the detector efficiency is accurately known as a function of source position and energy, if the counting geometry and the sample size and shape are accurately known, and if the gamma-ray emission rates are accurately known. However, it is tedious to characterize a detector efficiency with sufficient accuracy, and there are still significant uncertainties in the values of the specific activities for many important gamma rays. The use of calibration standards reduces or eliminates the need to accurately know the detector efficiency, the counting geometry, and the specific activities.

The most authoritative guide for calibrating NDA systems, ANSI N15.20-1975 (Ref. 1), rather firmly insists that a calibration standard is "an item physically and chemically similar to the items to be assayed," a restriction no longer necessary for gamma-ray assay. The guide also insists that calibration standards "must be chosen so that their contained masses of the nuclide(s) of interest span the mass range expected for the items to be assayed." This restriction may be considerably relaxed. Relatively few standards are usually needed to calibrate gamma-ray assay systems for the accurate assay of items covering a wide range of size, shape, chemical composition, and mass.

Sections 6.2 to 6.6 describe the nature and computation of the attenuation correction factor  $CF(AT)$ . A more detailed discussion of this subject is given in Ref. 2. Section 6.7 discusses calibration standards and Section 6.8 describes assay systems using transmission-corrected procedures.

## 6.2 PROCEDURES

### 6.2.1 Preliminary Remarks

The procedures and methods described herein are best applied with high-resolution gamma-ray detectors. The methods and correction factors may be used for assays with low-resolution detectors, but additional care must be exercised to avoid unnecessary error, and the ultimate accuracy will be not be as good.

The most unpleasant and important fact in applying gamma-ray spectroscopy is that the raw count rate for a given gamma ray is not usually proportional to the amount of the nuclide emitting the gamma ray. Two reasons for the lack of proportionality are the rate-related electronic processes of deadtime and pulse pileup and the self-attenuation of the sample. Accurate gamma-ray assays demand accurate corrections for both the electronic losses and the losses caused by sample self-attenuation. Corrections for electronic losses are described in detail in Chapter 5.

### 6.2.2 General Description of Assay Procedure

If the raw data-acquisition rate is multiplied by appropriate correction factors for both the rate-related electronic losses and the sample self-attenuation, we may write (as in Equation 5-60 of Section 5.4)

$$CR = RR \times CF(RL) \times CF(AT)$$

or

$$CR = FEIR \times CF(AT) \quad (6-1)$$

where CR = total corrected rate  
 RR = raw rate of data acquisition  
 CF(RL) = correction factor for rate-related electronic losses  
 CF(AT) = correction factor for self-attenuation in sample  
 FEIR = full-energy interaction rate.

If the correction factors are properly defined and computed, CR is the data-acquisition rate that would have been observed if there were no electronic losses and if the sample were changed to a simpler shape (such as a point or line) with no self-attenuation. Thus computed, CR is proportional to the mass of the isotope emitting the gamma ray of interest. We can then write

$$CR = K \times M \quad (6-2)$$

where M is the mass of the isotope being assayed and K is a calibration constant. The calibration constant K is determined by the use of appropriate standards and includes

the effects of detector efficiency, subtended solid angles, and gamma-ray emission rates. The CF(AT) is determined so that the CRs for both unknown and standard are those that would have been observed if they had had the same nonattenuating spatial configuration.

The above, in essence, constitutes a general approach to passive gamma-ray assay. The individual steps of this approach are

- (1) Measure the raw data-acquisition rate.
- (2) Determine the correction for rate-related electronic losses.
- (3) Determine the correction for gamma-ray self-attenuation.
- (4) Compute the total corrected rate, which is proportional to the mass of the isotope being assayed.
- (5) Determine the constant of proportionality, the calibration constant, by use of appropriate physical standards, making sure that the CR for both standards and unknowns represents the same nonattenuating geometrical shape in the same position with respect to the detector.

Both RR and CF(RL) are relatively easy to determine accurately and are discussed in detail in Chapter 5.

### 6.2.3 Necessary Assumptions for Determining the Self-Attenuation Correction Factor

In determining CF(AT), the basic question is, what fraction of the gamma rays of interest that are emitted in directions such that they could reach the detector actually do reach the detector? If the sample material can be characterized by a single linear attenuation coefficient  $\mu_\ell$ , the fraction of gamma rays that escape unmodified from the sample can, in general, be computed. Determining  $\mu_\ell$  is the key to determining CF(AT).

Two assumptions seem adequate to permit accurate gamma-ray assays:

- The mixture of gamma-ray-emitting material and matrix material is reasonably uniform and homogeneous in composition and density.
- The gamma-ray-emitting particles are small enough that the self-attenuation within the individual particles is negligible.

These assumptions guarantee that the linear attenuation coefficient is single-valued on a sufficiently macroscopic scale that it can be used to accurately compute the gamma-ray-escape fraction. There are no restrictions on the chemical composition of the sample. All that is required is that  $\mu_\ell$  can be computed or measured. Unknown samples need not have the same or even similar chemical compositions as the calibration standards. There are also no basic assumptions about the size and shape of standards, although there are limitations.

The assumption of "reasonable" uniformity is admittedly vague and difficult to define. What constitutes reasonable uniformity depends on the gamma-ray energy, the chemical composition of the sample, and the accuracy required. Some sample types almost always satisfy the assumptions and some almost never do so.

The mass attenuation coefficients  $\mu$  (Chapter 2) of the elements impose the fundamental restrictions on the size, shape, composition, and density of samples that can be successfully assayed by gamma-ray methods. Figure 6.1 shows mass attenuation coefficients for selected elements ranging from hydrogen ( $Z = 1$ ) to plutonium ( $Z = 94$ ). Qualitatively, the information in the graph defines nearly all the possibilities and limitations of passive gamma-ray NDA. Note that  $\mu$  for uranium at 185.7 keV is nearly six times larger than that for plutonium at 413.7 keV. This means that the assay of  $^{235}\text{U}$  by its 185.7-keV gamma ray is subject to considerably more stringent limitations on sample size, particle size, and uniformity than is the assay of  $^{239}\text{Pu}$

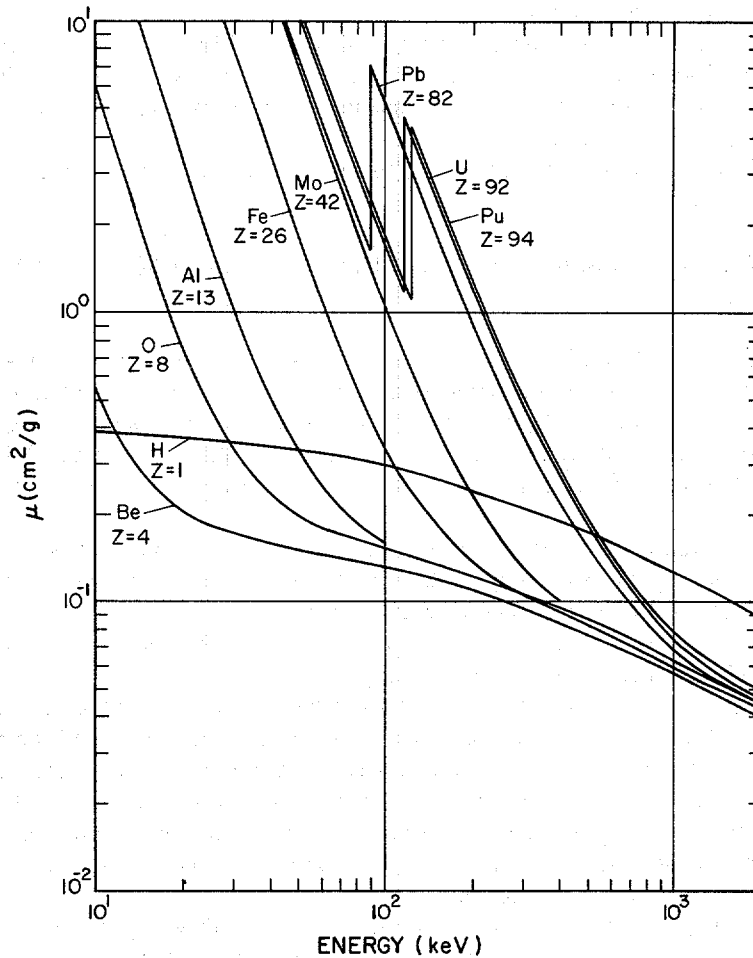


**Fig. 6.1** Total mass attenuation coefficients (without coherent scattering contribution) vs energy for nine elements ranging in atomic number  $Z$  from 1 to 94 (Ref. 3).

by its 413.7-keV gamma ray. Below  $\sim 80$  keV, the  $\mu$  of most elements rises rapidly, making attenuation problems unmanageably severe for all but small samples of very small particle size.

Figure 6.2 is given as an aid in estimating self-attenuation for individual particles.\* It gives the fraction of gamma rays escaping unscattered from spherical sources as a function of the product  $\mu\rho D$ , where  $D$  is the diameter of the sphere. As an example, for a 200- $\mu\text{m}$ -diameter,  $\rho = 10 \text{ g/cm}^3$  particle of  $\text{UO}_2$ ,  $\mu\rho D \simeq 0.28$ , indicating that  $\sim 10\%$  of the 185.7-keV gamma rays emitted are scattered with some energy loss or are completely absorbed within the particle.

Solutions meet the criteria for accurate gamma-ray assay, assuming that there are no contained particulates or precipitates. Pure powders ( $\text{PuO}_2$ ,  $\text{UO}_2$ ,  $\text{U}_3\text{O}_8$ , and so forth) almost always are suitable, as are certain well-mixed scrap materials such as incinerator ash. High-temperature gas reactor (HTGR) coated fuel particles and HTGR-type rods come close to meeting the requirements, but assay results are low by 5 to 10% unless correction is made for the self-attenuation in the particle kernels (Ref. 5). Small quantities of high-Z gamma emitters ( $< 10 \text{ g}$ ) mixed with low-Z,

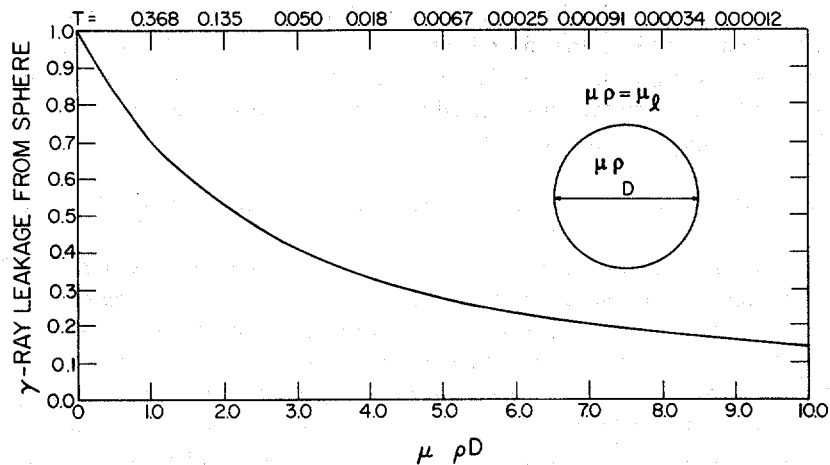


Fig. 6.2 Fraction of gamma rays escaping unscattered and unabsorbed from spherical sources as a function of  $\mu\rho D$ . Coherent (elastic) scattering has been neglected.

\* The expression for the fraction of gamma rays escaping unscattered and unabsorbed from a sphere whose attenuation properties are characterized by  $X = \mu\rho D$  is given by

$$F = \frac{3}{2X} \left[ 1 - \frac{2}{X^2} + \exp(-X) \left( \frac{2}{X} + \frac{2}{X^2} \right) \right]$$

For proof of this expression, see Ref. 4.

low-density combustibles may meet the requirement if there are no agglomerations of the powder with significant self-attenuation. Large quantities of high-Z powders (greater than about 100 g) will almost surely create some significantly attenuating agglomerations when mixed with such combustibles. Among the worst cases are metal chips of high-Z, high-density metals or fuel pellets mixed with low-Z, low-density matrices; in these situations assays may well be low by factors of 2 or 3 or even more. This fact causes one to be cautious about using gamma-ray methods to screen heterogeneous materials for possible criticality dangers.

It must be emphasized that the degree to which materials satisfy the two assumptions is the most important factor in determining the potential accuracy of a gamma-ray assay. Experience indicates, for example, that small samples of solution (up to a few tens of cubic centimeters) may be assayed with accuracies of a few tenths of a percent. Samples of uniform, homogeneous powders of volumes up to a few liters have been assayed with accuracies approaching 1% in spite of significant density gradients. Larger containers of waste (for example, 30-gal. drums) rarely satisfy the assumptions well enough to allow errors of <10%, and the error will be much worse for the extremely heterogeneous cases.

Another important general fact about gamma-ray assay is that the results are almost always low when samples that do not satisfy the assumptions are assayed in conjunction with calibration standards that do satisfy the assumptions. The procedures that accurately determine the self-attenuation in acceptable samples underestimate the correction in samples that fail to satisfy the required conditions.

#### 6.2.4 Methods for Determining the Sample Linear Attenuation Coefficient

Four principal methods have been employed to determine the sample  $\mu_\ell$  (Ref. 6). The oldest method avoids the issue by using representative standards. In this procedure a set of calibration standards are prepared as nearly identical as possible in size, shape, and composition to the unknowns. The standards are counted in a fixed geometry to prepare a calibration curve, and the assay is accomplished by counting the unknowns in the same geometry and comparing the count directly with the calibration curve. This procedure produces good results only if the unknowns and standards are sufficiently similar that the same concentration of assay material in each gives rise to the same  $\mu_\ell$  and, therefore, to the same CF(AT). The representative standard procedure also assumes that the pileup and deadtime losses are equal for equal concentrations of assay isotopes. This method is only applicable when the nature and composition of the assay samples are well known and essentially unvarying.

A second method exploits previous knowledge of the chemical composition, mass, and shape to compute  $\mu_\ell$ . Sufficient prior knowledge to compute the sample  $\mu_\ell$  does not necessarily mean that the assay result is known in advance. In many cases,  $\mu_\ell$  is almost purely dependent on the matrix composition and mass, which is reasonably well known. When only verification measurements are required on well-characterized materials, the approach is useful even when the assay material contributes significantly

---

to the sample self-attenuation. Computation of the sample  $\mu_\ell$  from knowledge of the chemical composition and densities is straightforward. References 3 and 7 tabulate the necessary mass attenuation coefficients.

Another method of determining CF(AT) involves measuring the intensity ratio of gamma rays of two different energies from the same isotope and comparing it with the same ratio from a thin source (negligible self-attenuation) containing the same isotope. This method is of limited use because, in general,  $\mu_\ell$  is not uniquely related to the measured intensity ratios. Some prior knowledge of the nature of the sample is also required to obtain the actual correction factors. Furthermore, not all isotopes have a pair of gamma rays of the appropriate energies. Nevertheless, the method has proved useful in specific cases and has the potential for giving warning when the assumptions on uniformity and particle size are grossly violated.

The fourth and most general method of obtaining  $\mu_\ell$  involves measuring the transmission through the sample of a beam of gamma rays from an external source. From the fundamental law of gamma-ray attenuation, the transmission is

$$T = \exp(-\mu_\ell x) \quad (6-3)$$

where  $x$  is the thickness of the sample. Solving for  $\mu_\ell$ , we obtain

$$\mu_\ell = \frac{-\ln(T)}{x} \quad (6-4)$$

This method requires no knowledge of the chemical composition or density of the sample, just the basic assumptions on uniformity and particle size. In fact, it is often the preferred method even when some knowledge of the sample composition is available, particularly when the best obtainable accuracy is desired. The experimentally measured  $\mu_\ell$  includes all the effects of chemical composition and density.

The transmission method can identify those samples for which accurate quantitative assays are impossible because of excessive self-attenuation. As the measured transmission decreases, its precision deteriorates along with the precision of the sample  $\mu_\ell$ , thus creating error in the computed value of CF(AT). The precision and accuracy of the measured transmission become unacceptable for transmissions between 0.01 and 0.001. Transmission values  $\leq 0.001$  (perhaps even negative) almost always indicate an unassayable sample.

## 6.3 FORMAL DEFINITION OF CORRECTION FOR SELF-ATTENUATION

### 6.3.1 The General Definition

Expressions for CF(AT) can be formulated in a number of useful ways. The formulation adopted here is a multiplicative correction factor that gives a corrected count rate that is directly proportional to the quantity of isotope being measured. It is useful

---

to define CF(AT) with respect to a specified geometrical shape, which is often simpler than the actual shape.

$$CF(AT) = \frac{FEIR(\mu_{\ell} = 0; \text{Specified Shape})}{FEIR(\mu_{\ell} \neq 0; \text{Real Shape})} \quad (6-5)$$

where  $FEIR(\mu_{\ell} = 0, \text{Specified Shape}) =$  the FEIR that would have been measured if the sample were totally nonattenuating ( $\mu_{\ell} = 0$ ) and if it were changed to the specified shape  
 $FEIR(\mu_{\ell} \neq 0, \text{Real Shape}) =$  the actual measured FEIR from the sample.

In practice, CF(AT) is not computed from Equation 6-5; it is determined from  $\mu_{\ell}$ , the geometrical configuration, and the position of the sample relative to the detector. Most often the expressions for CF(AT) are not integrable in terms of elementary functions, so numeric methods must be used.

Generally, the detector efficiency need not be known. Usually one can assume a point detector with equal efficiency for all angles of incidence, which considerably simplifies the computations. This assumption is usually good when the distance between sample and detector is at least several times the maximum dimension of either the detector or the sample. If the sample-to-detector distance must be kept small for reasons of efficiency and if the highest obtainable accuracy is required, the actual measured or calculated detector efficiency as a function of energy and position may be used. Cline (Ref. 8) describes a procedure for creating an efficiency function based on measurements of standard sources, which should be adequate for almost all requirements.

### 6.3.2 Useful Specified Shapes

The most useful specified shapes are

- the actual sample shape
- a point
- a line.

If one has many samples and standards of the same shape and size, then CF(AT) may be computed with respect to a nonattenuating sample of the same shape. When the sample is sufficiently uniform and homogeneous and of reasonable size, let the detector view the whole sample and use the CF(AT) computed with respect to a nonattenuating point. This allows the standards and the unknowns to be of different size, shape, and chemical composition. However, for such assays to be accurate, the entire contents must be reasonably well represented by a single  $\mu_{\ell}$ .

Samples often have vertical composition and density gradients, the natural consequence of filling relatively narrow containers from the top. The material tends to fall into the containers in layers. In such cases, a single  $\mu_{\ell}$  cannot adequately characterize the whole sample, but narrow layers or segments can be adequately characterized by



a single  $\mu_\ell$  value. The assay accuracy can be improved by using a segmented scan in which the detector views the sample through a collimator that defines relatively narrow horizontal segments in which  $\mu_\ell$  can be assumed constant. For such segmented scans, it is best to compute the CF(AT) with respect to a nonattenuating line along the axis of the containers. In this way, cylindrical samples may be accurately assayed with respect to standards of quite different diameters.

#### 6.4 IMPORTANT PARAMETERS OF THE SELF-ATTENUATION CORRECTION FACTOR

The correction factor for self-attenuation, CF(AT), is a function of many parameters. Those currently recognized as significant are listed below in decreasing order of importance:

- the  $\mu_\ell$  of the sample material
- the volume and shape of the sample material
- the  $\mu_\ell$  of the sample container
- the size and shape of the sample container
- the position and orientation of the sample relative to the detector
- the size, shape, and efficiency of the detector.

In many situations the dependence of CF(AT) on several of the parameters is mild. For example, when the sample-to-detector distance is at least several times the maximum dimensions of the detector, the dependence of CF(AT) on the size, shape, and efficiency of the detector is often negligible. When the distance between a cylindrically shaped sample and the detector is at least several times the maximum dimension of either sample or detector, CF(AT) is usually a strong function of the sample  $\mu_\ell$ , a mild function of the sample dimensions and distance from the detector, and has negligible dependence on the detector size, shape, and efficiency.

The greatest simplifications occur in the far-field case, where the maximum dimensions of both sample and detector are negligible compared with their separation. In the far-field case, dependence on the inverse-square law becomes negligible and all gamma rays reach the detector along essentially parallel paths. There is no dependence on detector size or shape, on small changes in the sample-to-detector distance, or on sample size except for the influence of size on the fraction of gamma rays escaping from the sample. Simple analytic expressions can be derived for several sample shapes. These expressions are often useful approximations for assay situations that are not truly far field. Indeed, the far-field situation is a useful reference case against which to compare near-field cases.

It is usually advantageous to plot CF(AT) vs the parameter of strongest dependence ( $\mu_\ell$ ) and to plot separate curves for specific values of other parameters. Because  $\mu_\ell$  is often found by measuring the gamma-ray transmission T and using the relationship  $T = \exp(-\mu_\ell x)$ , it is generally more convenient to plot CF(AT) vs  $\ln(T)$ .

Consider the expression for CF(AT) for the far-field assay of a box-shaped sample viewed normal to a side.

---

$$CF(AT) = \frac{\mu \rho x}{[1 - \exp(-\mu \rho x)]} \quad (6-6)$$

where  $x$  is the sample thickness along the normal to the detector. Using  $T = \exp(-\mu \rho x)$ , we can write the simple expression

$$CF(AT) = \frac{-\ln(T)}{(1 - T)}. \quad (6-7)$$

If  $T \ll 1$ ,  $CF(AT) \approx -\ln(T)$ , so a plot of  $CF(AT)$  vs  $\ln(T)$  is nearly linear. Figure 6.3 gives a plot of Equation 6-7. It also shows  $CF(AT)$  vs  $\ln(T)$  for cylindrical and spherical samples where  $T$  is measured across the sample diameter. All the cases have the form  $CF(AT) \approx -k \ln(T)$  for  $T \ll 1$ . This approximate  $\ln(T)$  dependence exists for most assay geometries and is very useful to keep in mind.

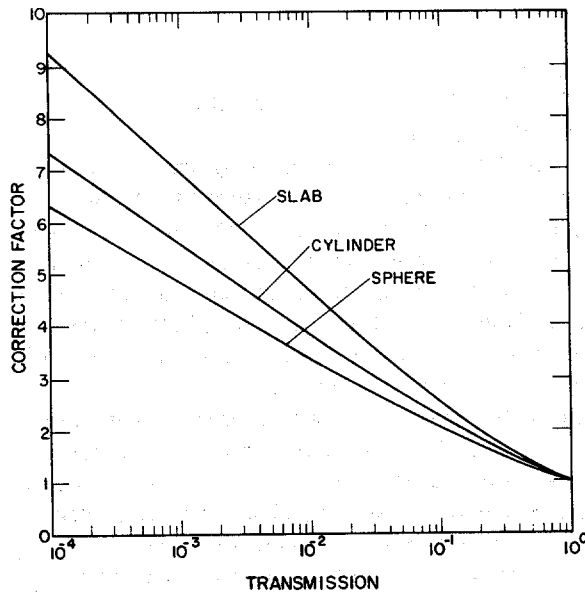


**Fig. 6.3** Far-field correction factors for slab, cylindrical, and spherical samples as a function of transmission. The transmission is measured normal to the face of the slab sample and along a diameter of the cylindrical and spherical samples.

## 6.5 ANALYTIC FAR-FIELD FORMS FOR THE SELF-ATTENUATION CORRECTION FACTOR

In general, the near-field integral expressions for  $CF(AT)$  cannot be integrated in terms of elementary functions. However, far-field expressions have been derived for

three simple sample geometries: box shaped (rectangular parallelepipeds), cylindrical, and spherical. Figure 6.3 gives the far-field CF(AT) for all three sample shapes, and Table 6-1 gives numeric values for the three cases.

Table 6-1. Far-field correction factors for slab, cylinder, and sphere as functions of transmission

Transmission	Slab <sup>a</sup>	Cylinder <sup>b</sup>	Sphere <sup>b</sup>
1.0000	1.000	1.000	1.000
0.8000	1.116	1.097	1.086
0.6000	1.277	1.231	1.202
0.4000	1.527	1.434	1.376
0.2000	2.012	1.816	1.701
0.1000	2.558	2.238	2.054
0.0500	3.153	2.692	2.431
0.0200	3.992	3.326	2.956
0.0100	4.652	3.826	3.370
0.0010	6.915	5.552	4.805
0.0001	9.211	7.325	6.288

<sup>a</sup>Transmission normal to surface.

<sup>b</sup>Transmission along a diameter.

### 6.5.1 Box-Shaped Samples

The box-shaped sample is the only one for which a simple derivation exists. From Equation 6-5, we can write CF(AT) with respect to a nonattenuating sample (specified shape same as real shape) as

$$CF(AT) = \frac{\int_v \rho I \varepsilon \, dV}{\int_v \rho I \varepsilon \exp(-\mu_\ell r) \, dV} \quad (6-8)$$

- where
- $\rho$  = spatial density of the isotope being assayed (g/cm<sup>3</sup>)
  - $I$  = emission rate of the assay gamma ray ( $\gamma$ /g-s)
  - $\varepsilon$  = absolute full-energy detection efficiency
  - $\mu_\ell$  = linear attenuation coefficient of the sample
  - $r$  = distance that gamma rays travel within the sample
  - $dV$  = volume element.

The parameters  $\rho$ ,  $I$ , and  $\mu_\ell$  are constant, whereas  $\varepsilon$  and  $r$  are functions of position. It is the exponential term in the denominator that, for most geometrical configurations, cannot be integrated in terms of elementary functions.

Consider the configuration shown in Figure 6.4. The parameter  $I$  is a constant for a given isotope, and by virtue of the fundamental assumptions on uniformity,  $\rho$  and  $\mu_\ell$  are also constant. The far-field assumption is equivalent to assuming that  $\epsilon$  is also a constant.

Because of the far-field assumption, only the integration in  $X$  is significant. After the obvious cancellations,

$$CF(AT) = \frac{\int_0^X dx}{\int_0^X \exp[-\mu_\ell(X-x)] dx} \quad (6-9)$$

This evaluates to

$$CF(AT) = \frac{\mu_\ell X}{1 - \exp(-\mu_\ell X)} \quad (6-10)$$

as in Equation 6-6.

### 6.5.2 Cylindrical Samples

For a cylindrical sample viewed along a diameter in the far field (Ref. 9),

$$CF(AT) = \frac{1}{2} \frac{\mu_\ell D}{I_1(\mu_\ell D) - L_1(\mu_\ell D)} \quad (6-11)$$

where  $L_1$  = modified Struve function of order 1

$I_1$  = modified Bessel function of order 1

$D$  = sample diameter

$\mu_\ell$  = linear attenuation coefficient of the sample.

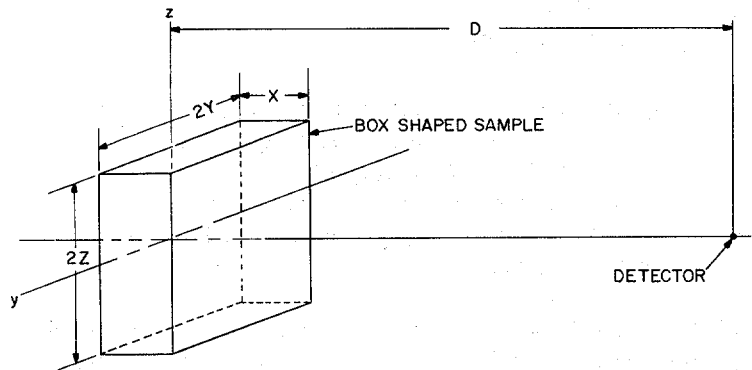


Fig. 6.4 Counting geometry for a slab-shaped sample with coordinates and dimensions for use in deriving the far-field correction factor.

The expression is very compact, but it is inconvenient to use because of the Struve and Bessel functions (Ref. 10). Equation 6-11 was used to generate the curve for a cylinder in Figure 6.3. Note that the CF(AT) for a cylinder is a little less than those for a slab or box-shaped sample. In the cylindrical sample, fewer gamma rays must penetrate the maximum thickness of material; hence, the fraction escaping is greater and the CF(AT) is smaller.

### 6.5.3 Spherical Samples

For a spherical sample in the far field, the correction factor is (Ref. 4)

$$\text{CF(AT)} = \left( \frac{3/2}{\mu \ell D} \left\{ 1 - \frac{2}{(\mu \ell D)^2} + \exp(-\mu \ell D) \left[ \frac{2}{\mu \ell D} + \frac{2}{(\mu \ell D)^2} \right] \right\} \right)^{-1} \quad (6-12)$$

This expression is plotted in Figure 6.3. The CF(AT) for a sphere is smaller than that for either the parallelepiped or cylinder. On the average, gamma rays travel shorter distances to escape from a sphere than from either a cylinder or a cube. Spherical samples are rarely met in practice, but the reciprocal of CF(AT) gives the fraction of gamma rays escaping from spherical particles and is useful in deciding whether a sample meets the required assumption on particle size. Figure 6.2 was generated from Equation 6-12.

## 6.6 NUMERIC COMPUTATION IN THE NEAR FIELD

### 6.6.1 General Discussion

For most if not all near-field situations in which the inverse-square dependence must be treated explicitly, the resulting expressions cannot be integrated in terms of elementary functions. As a result, numeric methods must be used, which implies the use of computers. However, even with the power of modern computers, the simplest model should be used to describe the assay situation. It is often possible to simplify the computations by assuming a point or line detector with efficiency independent of angle of incidence. For complicated geometries, Monte Carlo photon transport codes can be used. However, the NDA situations can usually be handled with simplified models and straightforward one-, two-, or three-dimensional numeric integration methods using simple codes and small computers. The accuracy of gamma-ray NDA is usually determined more by the sample uniformity and homogeneity than by the accuracy of the CF(AT) computation.

Approximate analytic forms exist that give adequately accurate values for CF(AT) over reasonable ranges of transmission. A few such forms are described below. The adequacy of a particular expression can be determined by comparison with more accurate numeric computations. Approximate analytic forms often provide the capability to derive analytic expressions for the precision of CF(AT).

### 6.6.2 A Useful One-Dimensional Model

A common assay geometry is that in which a germanium detector views a bottle of solution from below. Both detector and sample are well approximated by right-circular cylinders. Assume that the axes of symmetry of the bottle and the detector coincide and that the detector radius is  $r_d$ , the sample radius is  $r_s$ , the sample depth is  $D$ , and the distance from sample to detector is  $d$  (Figure 6.5). If  $d$  is a few times greater than both  $r_d$  and  $r_s$ , no gamma ray impinges on the detector at angles greater than  $\sim 10^\circ$  to the common axis. Inasmuch as  $\cos \Theta \geq 0.95$  for angles  $< 19^\circ$ , it is clear that no gamma ray travels more than a few percent greater distance on its way to the detector than those that travel parallel to the common centerline. Therefore, the assay situation can be described by a one-dimensional model consisting of a point detector and a line sample of "depth"  $D$  and linear attenuation coefficient  $\mu_l$  separated from the detector by a distance  $d$  as indicated in Figure 6.6. This model contains the effects of the inverse-square law and gamma-ray attenuation, which are the main influences on the  $CF(AT)$ .

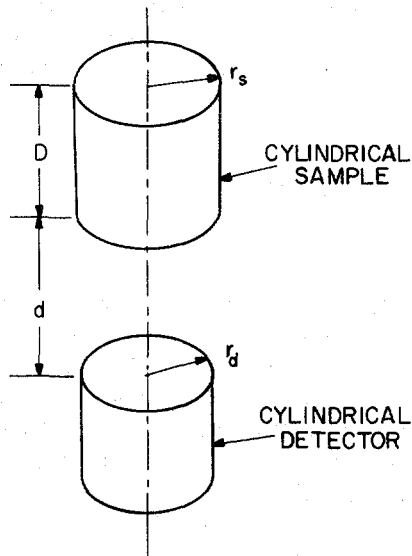


Fig. 6.5 Commonly used vertical assay geometry for which a one-dimensional model is appropriate for computing  $CF(AT)$ .

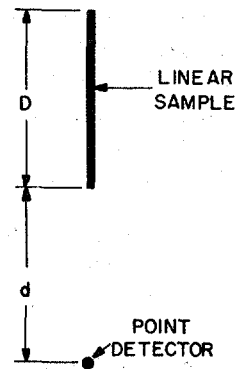


Fig. 6.6 One-dimensional model for computing  $CF(AT)$ .

Using this model, CF(AT) with respect to a nonattenuating sample is

$$\text{CF(AT)} = \left[ \int_0^D \frac{dx}{(d+x)^2} \right] / \int_0^D \frac{[\exp(-\mu_\ell x)] dx}{(d+x)^2} \quad (6-13)$$

where all constants pertaining to the detector efficiency and gamma-ray emission rates have cancelled. The numerator integrates to  $D/[d(d+D)]$ , but as simple as the denominator appears to be, it cannot be integrated in terms of elementary functions. However, it can be written as a sum in a simple way. The expression for CF(AT) then becomes

$$\text{CF(AT)} = \left[ \frac{D}{d(d+D)} \right] / \sum_{I=1}^N \frac{\{\exp[-\mu_\ell(I-0.5)\Delta x]\} \Delta x}{[d+(I-0.5)\Delta x]^2} \quad (6-14)$$

where  $\Delta x = D/N$  and  $N$  is the number of intervals for the numeric integration. Generally, taking  $N \simeq 100$  gives the result to  $<0.1\%$ . The numeric integration could, of course, be done with better accuracy and in fewer steps using Simpson's rule or other more elegant methods. Equation 6-14 shows clearly the functional dependence of CF(AT) on  $d$ ,  $D$ , and  $\mu_\ell$  and the equivalence of the integral and the sum. The parameter  $D$  is well defined as the sample depth. The parameter  $d$ , however, is less well defined because the gamma rays interact throughout the detector and because the average interaction depth is a function of energy. Experience shows that if the nominal value of  $d$  is at least a few times  $D$ , then with the help of a set of standards covering a wide range of  $\mu_\ell$ , the value of  $d$  in Equation 6-14 can be adjusted to give CF(AT) such that the corrected rate per unit activity is nearly constant over a wide range of  $\mu_\ell$ . The adjustment of  $d$  compensates for the imprecisely known sample-to-detector distance and for deviation of the one-dimensional model from the actual three-dimensional assay geometry.

Figure 6.7 shows results of a measurement exercise using the procedure just described. The samples were 25-mL solutions of depleted uranium nitrate in flat-bottomed bottles of  $10 \text{ cm}^2$  area (right-circular cylinders 3.57 cm in diameter and 2.5 cm deep). The uranium concentration varied from 5 to 500 g/L, and all the samples were spiked with an equal amount of  $^{75}\text{Se}$ ;  $^{75}\text{Se}$  was the source material, uranium served as an absorber only. The detector crystal was  $\sim 4.0$  cm in diameter and  $\sim 4.0$  cm long. For the 136.0-keV gamma ray of  $^{75}\text{Se}$ , the corrections for electronic losses, CF(RL), varied by only  $\sim 10\%$ , whereas the corrections for gamma-ray attenuation, CF(AT), varied by  $\sim 275\%$ .

Because each sample had identical amounts of  $^{75}\text{Se}$ , the corrected 136.0-keV rate should have been equal for all samples. The upper part of the figure gives the fractional deviation of the corrected rates from the average of all and indicates the typical precision of the measurements. All the corrected rates are within about  $\pm 0.5\%$  of the average. In this case, the actual distance of the sample bottom to the average

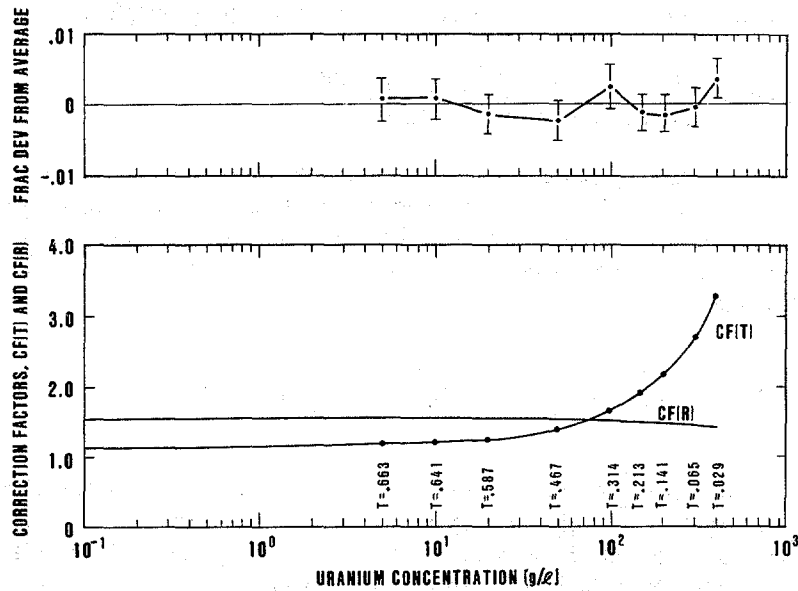


Fig. 6.7 Results of a measurement exercise designed to test the usefulness of a one-dimensional model for computing  $CF(AT) = CF(T)$ .

interaction depth in the detector was  $\sim 8$  cm and the adjusted value was 9.0 cm. Qualitatively, the one-dimensional model gives values of  $CF(AT)$  that are a little low compared with the correct three-dimensional model because the gamma rays pass through slightly greater thicknesses of solution than in the one-dimensional model. Increasing  $d$  increases  $CF(AT)$  overall and also increases  $CF(AT)$  more for lower values of  $T$ . Hence, the value of  $d$  used in computations is usually a little higher than the physical value.

If a set of solution samples has variable but determinable depths, one would prefer to compute  $CF(AT)$  with respect to a nonattenuating point so that the corrected rates from all the samples can be compared directly. The ratio between  $CF(AT)$  with respect to the nonattenuating point and  $CF(AT)$  with respect to the nonattenuating sample is  $(1 + D/d)$ , independent of  $\mu\rho$ . All  $CF(AT)$  values, for both standards and unknowns, should be computed with respect to the same nonattenuating shape so that the corrected rates are directly comparable.

### 6.6.3 A Useful Two-Dimensional Model

In another common assay geometry, a detector views a cylindrical sample from the side (Figure 6.8). If the sample depth is less than the sample diameter and if the distance from the detector to the sample center is at least several times the sample diameter, then a simple two-dimensional model can often be used to compute  $CF(AT)$ .



The model is a point detector at a distance  $D$  from the center of a circular sample of radius  $R$  (Figure 6.9). The detector efficiency is essentially constant for gamma rays originating at any point within the sample volume. The correction factor with respect to the nonattenuating sample can be written as

$$CF(AT) \approx \frac{(\pi/2)\ln[1 - R^2/D^2]}{\sum_{m=1}^M \sum_{n=1}^N \{\exp[-\mu_{\rho}t(m,n)]\Delta A(n)/L^2(n,m)\}} \quad (6-15)$$

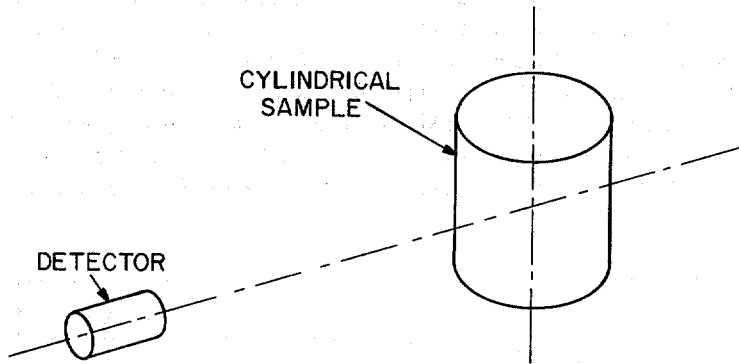


Fig. 6.8 Typical assay geometry for which a two-dimensional model for computing  $CF(AT)$  is usually adequate.

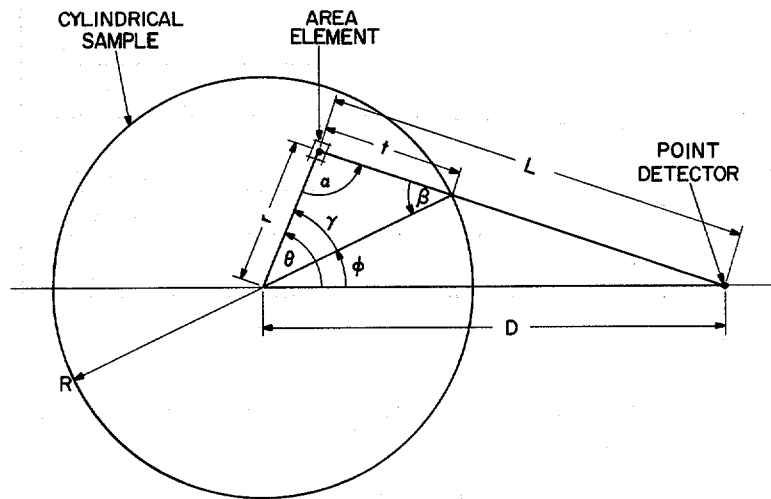
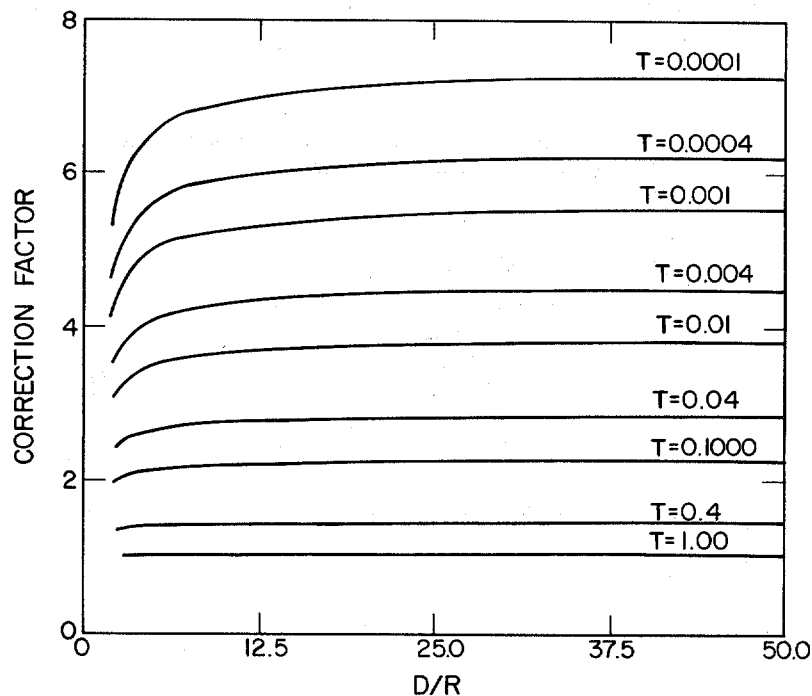


Fig. 6.9 Two-dimensional model for computing  $CF(AT)$  showing the distances that must be determined and the variables in terms of which they must be expressed. Note that  $0 \leq \alpha \leq \pi$ ,  $\beta \leq \pi/2$ , and  $0 \leq \gamma \leq \pi$ .

The derivation of this expression is given in Ref. 2. The ratio of  $CF(AT)$  calculated relative to the nonattenuating sample and  $CF(AT)$  calculated relative to a nonattenuating point is  $-(D^2/R^2) \ln(1 - R^2/D^2)$ . For a fixed value of  $T$ ,  $CF(AT)$  is a function only of the ratio  $D/R$ . Figure 6.10 gives  $CF(AT)$  as a function of  $D/R$  for several values of  $T$ . The essential point is that  $CF(AT)$  decreases slowly as  $D/R$  decreases; the larger changes occur for the smaller values of  $T$ . This behavior is a consequence of the inverse-square law. For a given value of  $T$ ,  $CF(AT)$  asymptotically approaches a maximum as  $D/R \rightarrow \infty$ . The deviations from the far-field ( $D/R = \infty$ ) case are plotted in Figure 6.11. For  $T > 0.001$  and  $D/R > 50$ , all deviations are  $\leq 1\%$ . Therefore,  $D/R \geq 50$  can be regarded as the far-field situation for most purposes. The variation of  $CF(AT)$  with  $T$  is much stronger than the variation with the ratio  $D/R$ .

The results presented in Figures 6.10 and 6.11 were obtained with a minicomputer using values of  $M = 200$  and  $N = 200$  for which all the results are within 0.1% of what the actual integrals would give. The total number of area elements computed was 40 000, and the time required was  $\sim 2$  min per value. The exact time required



**Fig. 6.10** Correction factors with respect to a nonattenuating sample as computed from the two-dimensional model. They are plotted vs the ratio  $D/R$  for various values of the transmission  $T$ , where  $D$  is the distance from the center of the cylindrical sample to the point detector and  $R$  is the radius of the sample.

depends greatly on the computing equipment and programming language used. For two-dimensional numeric integrations, results of high accuracy can be obtained in about a minute. For a three-dimensional model, a modest extension in derivation and programming, if the third dimension is also given 200 increments, the required execution time increases to hundreds of minutes.

#### 6.6.4 A Three-Dimensional Model

As a final model for an assay geometry, consider the segmented assay of cylindrical samples. In this case (Figure 6.12), a detector views the sample through a horizontal collimator, which defines sample segments that are assayed individually. The sample is usually as close to the collimator as possible. The detector is often a right-circular cylinder of germanium  $\sim 5.0$  cm in diameter and  $\sim 5.0$  cm long. The inverse-square-law effects caused by the collimator must be considered explicitly; the two-dimensional model is not adequate.

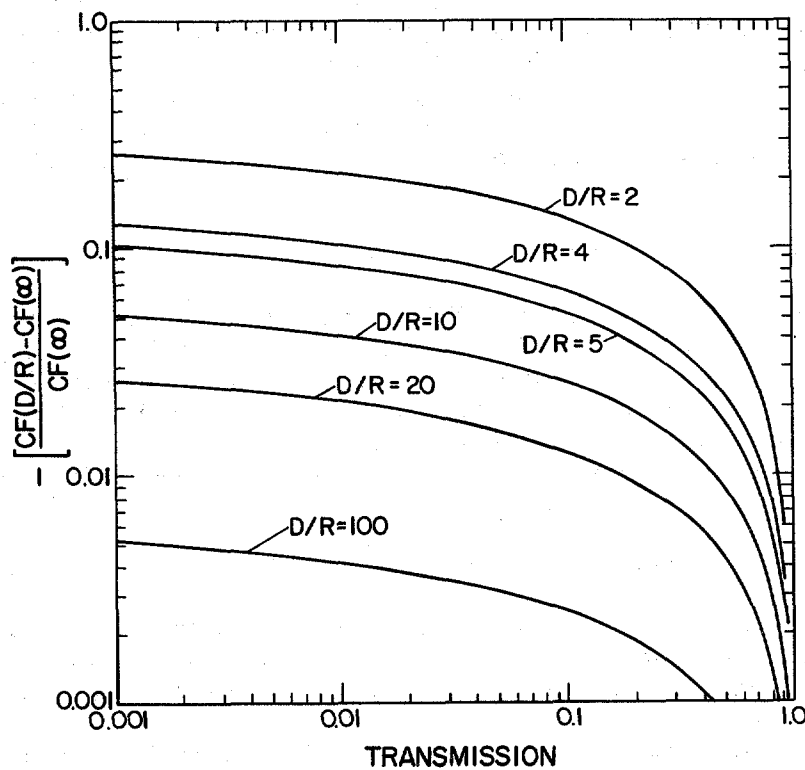
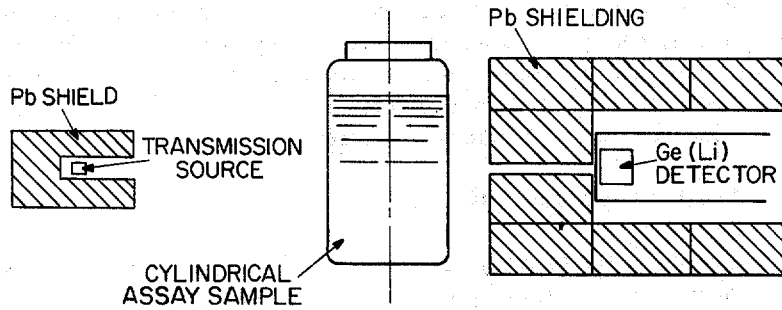


Fig. 6.11 Deviations of near-field values of  $CF(AT)$  from the far-field values as a function of transmission for various values of  $D/R$ .



*Fig. 6.12 Typical segmented assay situation for which a three-dimensional model for computing  $CF(AT)$  is appropriate.*

The model consists of a perfect collimator (no leakage) and a vertical line detector centered at the rear of the collimator. The detector efficiency is assumed to be independent of either the position or angle at which the gamma rays strike the line detector. The distance from the emitting element to the detector is increased by a constant that is approximately equal to the average interaction depth in the detector. Inasmuch as materials are often packaged in metal containers that significantly attenuate the emitted gamma rays, the packaging is included in the model. The derivation of the three-dimensional model is outside the scope of this text; it is treated fully in Ref. 2.

#### 6.6.5 Approximate Forms and Interpolation

The most accurate way to compute  $CF(AT)$  for reasonable assay geometries is to use a simple mathematical model and numeric integration. However, because of lengthy execution times, it is often desirable to compute  $CF(AT)$  for a few values of  $T$  (or  $\mu\ell$ ) and to use an interpolation scheme to find  $CF(AT)$  for intermediate values. The interpolation problem can be approached in several ways.

Since  $CF(AT)$  has an approximate  $\log(T)$  dependence (see Figure 6.3), it is reasonable to use a fitting function of the form

$$CF(AT) = A + B \log(T) + C [\log(T)]^2. \quad (6-16)$$

The computer need only store the constants  $A$ ,  $B$ , and  $C$  for each assay geometry. This scheme works very well over wide ranges of  $T$ . In a typical segmented scanning situation,  $A$ ,  $B$ , and  $C$  can be determined to give values of  $CF(AT)$  correct to  $\leq 0.3\%$  for  $0.008 \leq T \leq 0.30$ .

A particularly simple scheme is based on the far-field form of  $CF(AT)$  for a slab:  $-\ln(T)/(1 - T)$ . Observing that a circle is not very different from a square (see Figure 6.3), one is led to try

$$CF(AT) \simeq \frac{-\ln(T^k)}{(1 - T^k)} \quad (6-17)$$

with  $k < 1$  as an approximate function for cylindrical samples, even in the near-field situation. This form also has a  $\ln(T)$  dependence for  $T \ll 1$  and has only one constant to be determined. Figures 6.13 and 6.14 provide a feeling for how accurate the approximate form might be. Figure 6.13 gives the fractional deviation of Equation 6-17 from the correct far-field values for a cylinder (Equation 6-11) as a function of  $T$  and  $k$ . Figure 6.14 compares the approximate and correct values for a near-field assay of a cylindrical sample where  $D/R = 5/1$ . In Figure 6.13,  $k = 0.82$  gives  $CF(AT)$  correct within  $\pm 1\%$  for  $0.01 \leq T \leq 1.0$ , and in Figure 6.14,  $k = 0.75$  gives  $CF(AT)$  correct within  $\pm 1.5\%$  for  $0.01 \leq T \leq 1.0$ .

The choice of an interpolation procedure or approximate function for  $CF(AT)$  depends on the accuracy desired or possible for the materials to be assayed. For a field measurement of a heterogeneous drum containing  $^{235}\text{U}$ , the accuracy is determined far more by the heterogeneity of the sample material than by the function used for  $CF(AT)$ . When  $\pm 25\%$  accuracy is all that can be hoped for, it is wasteful to set up a model and do numeric integrations for  $CF(AT)$ . On the other hand, if the samples are solutions, where careful modeling and computation can yield accuracies  $< 1\%$ , the effort is fully justified.

#### 6.6.6 The Effects of Absolute and Relative Error in the Self-Attenuation Correction Factor

It is assumed that gamma-ray assay systems are calibrated with suitable physical standards. It is also assumed that  $CF(AT)$  is determined for both the unknowns and the standards. Generally,  $CF(AT)$  is mainly a function of the measured transmission  $T$  with some influence from the geometrical parameters.

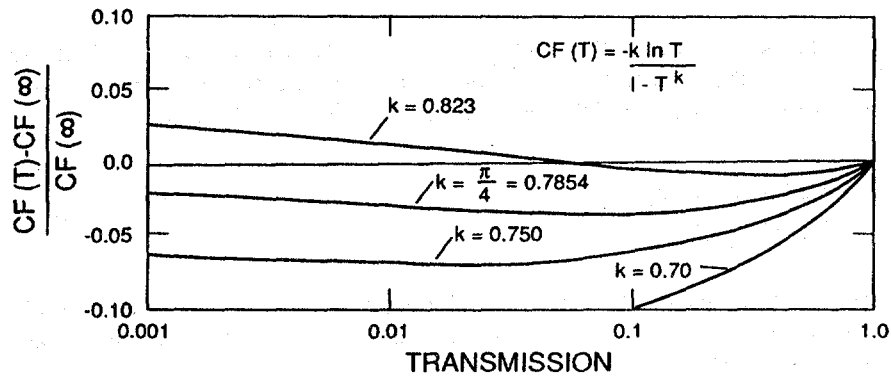


Fig. 6.13 Deviations of the values of  $CF(AT)$  computed from the approximate expression  $CF(T) = -k \ln T / (1 - T^k)$  from the far-field values for a cylinder for several values of the parameter  $k$ .

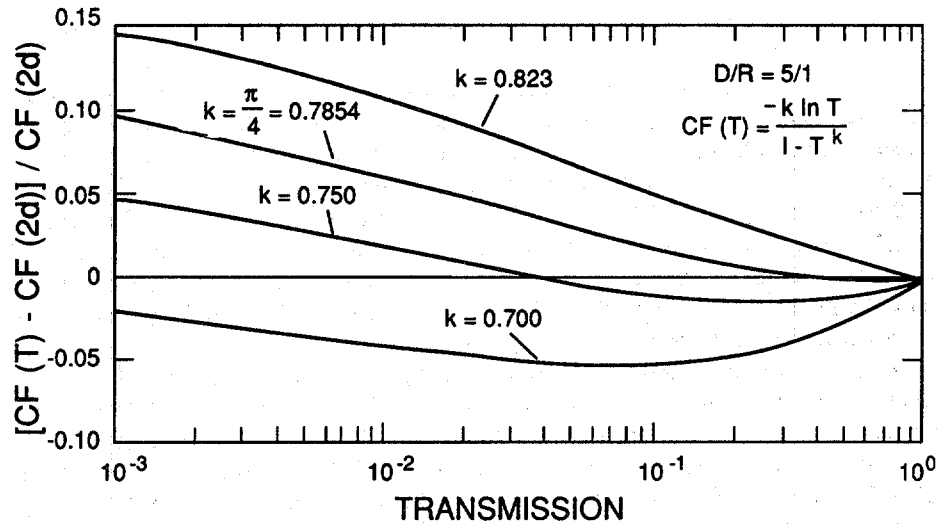


Fig. 6.14 Deviations of the values of  $CF(AT)$  computed from the approximate expression  $CF(T) = -k \ln T / (1 - T^k)$  from the values from the two-dimensional model for cylindrical samples for  $D/R = 5$ . They are plotted as functions of the transmission  $T$  for several values of the parameter  $k$ .

The consequences of using an incorrect function for  $CF(AT)$  should be investigated. Figure 6.15 shows a true and a false  $CF(AT)$  function. Let the following notation be adopted:

$$CF(T) = CF(AT) \text{ as a function of } T$$

$$G = \text{mass of assay isotope in unknown.}$$

The superscripts  $f$  and  $t$  indicate quantities associated with the false and true functions for  $CF(AT)$ , and the subscripts  $u$  and  $s$  indicate quantities associated with the unknown and the standard. The ratio of the incorrect result to the correct result is

$$\frac{G^f}{G^t} = \frac{CF^f(T_u)/CF^t(T_u)}{CF^f(T_s)/CF^t(T_s)} \quad (6-18)$$

The ratio does not depend directly on the absolute error in  $CF(T)$  but only on a ratio of ratios. If this ratio of ratios is  $\sim 1.00$ , the assays will be correct in spite of any absolute error in  $CF(AT)$ .

This result demonstrates that it is easier to calibrate an assay system correctly for a narrow range of transmission (which usually implies a narrow range of concentration of the assay isotope) than for a broad range. It also emphasizes that great care must

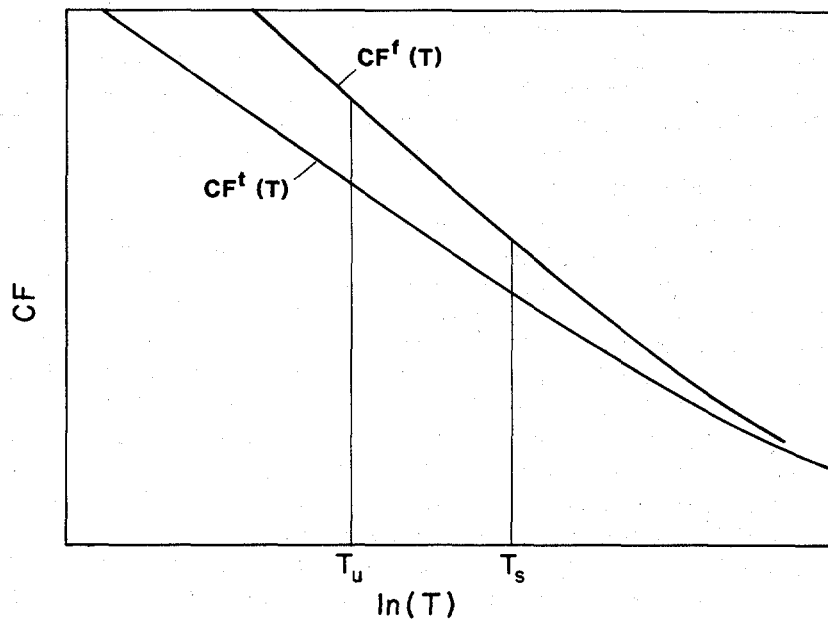


**Fig. 6.15** This graph can be used to illustrate the consequences of using an incorrect function for  $CF(AT)$ .  $CF^f(T)$  represents the incorrect or false function for  $CF(AT)$  and  $CF^t(T)$  represents the correct function.  $T_u$  and  $T_s$  represent the transmissions of unknown and standard, respectively.

be used in modeling the assay geometry and computing  $CF(AT)$  if high accuracy is required over a wide range of concentrations.

Considering the difficulty in computing  $CF(AT)$ , why not use standards to determine a variable calibration constant as a function of  $T$ ? Indeed that can be done, but preferably only as a fine tuning of a system calibration. A variable calibration constant or nonlinear calibration curve only sweeps under the rug the things that are not understood about the physics of the assay arrangement.

### 6.6.7 Precision of Self-Attenuation Correction Factor and Total Corrected Rate

In a properly operating gamma-ray NDA system, the precision is almost totally a function of the random nature of the emission and detection of the gamma rays. The influence of electronic fluctuations and drifts should almost never influence the precision of the results at a level  $>0.1\%$ . The dominant statistical component of the assay precision can usually be estimated from the full-energy peak areas and their precisions. The overall precision, including any contribution from the equipment, is estimated from replicate assays. The electronic and mechanical stability of the assay system can be evaluated by comparing the overall precision with that estimated from peak areas and their precisions.

Consider the influence of the precision of CF(AT) on the precision of the final assay. The assay is proportional to CR, which is given (see Equation 6-1) as  $CR = FEIR \times CF(AT)$ . The procedures used to derive expressions for  $\sigma(CR)$ ,  $\sigma(FEIR)$ , and  $\sigma[CF(AT)]$  are covered in detail in many sources (two relatively simple sources are Refs. 11 and 12). The intent here is only to emphasize a few points relative to obtaining a reasonable expression for  $\sigma(CR)$ .

If CR can be written as an analytic function of the peak areas, then an expression for  $\sigma(CR)$  can be derived. However, when CF(AT) is found by numeric procedures,  $\sigma(CR)$  cannot be computed directly. An approximate function for CF(AT) can be used to derive an expression for  $\sigma(CR)$ . The approximate forms for CF(AT) are often not sufficiently accurate to compute CR, but they usually provide an adequate expression for  $\sigma(CR)$ . In Section 6.6.2 a one-dimensional model was used to determine CF(AT) for the assay of cylindrical samples. To derive an expression for  $\sigma(CR)$ , one could use Equation 6-7 or the modified form Equation 6-17 for CF(AT). The proper value of k would be chosen by comparison with precisions computed from replicate assays. This procedure gives the accuracy provided by numeric integration of a more accurate model for CF(AT) and still provides good estimates of  $\sigma(CR)$ .

Although  $\sigma(CR)$  is the assay precision,  $\sigma[CF(AT)]$  alone is sometimes of interest. The expression for  $\sigma[CF(AT)]$  will always be simpler than that for  $\sigma(CR)$ . If no peak areas are common to the expressions for FEIR and CF(AT), then

$$\sigma_r(CR) = \sqrt{\sigma_r^2(FEIR) + \sigma_r^2[CF(AT)]} \quad (6-19)$$

where  $\sigma_r(x) \equiv \sigma(x)/x$ . If there are peak areas common to the expressions for FEIR and CF(AT), Equation 6-19 is not valid, and the expression for CR must be written as an explicit function of the peak areas concerned. Expressions for precision are frequently complex, but considerable simplification can usually be achieved by judicious approximations. The effort to make such simplifications reduces the computation time and provides a better understanding of the main source of imprecision.

## 6.7 FACTORS GOVERNING THE REQUIRED NUMBER OF STANDARDS

The current insistence that the mass range in NDA standards span the expected range in the unknowns can be considerably relaxed. The evidence for this allegation is implicit in the foregoing sections.

The insistence that the standards span the range of expected masses seems rooted in the expectation that a nonlinear calibration function will be fitted to the measured response data. For gamma-ray NDA systems, those response data might be RR or FEIR. Such plots are quite nonlinear, and extrapolation of a nonlinear function beyond the data points is not particularly safe. However, if the multiplicative correction factors CF(RL) and CF(AT) are properly defined and computed, a total corrected rate is obtained, which is a linear function of mass. If the calibration function is linear



(Equation 6-2), extrapolation is far less hazardous than with the nonlinear calibration functions, and most of the logical force is taken from the requirement that the mass range of the standards span that of the unknowns.

With Equation 6-2, the calibration constant,  $K$  can be determined with a single standard. However, it is wise to use several standards, spanning a reasonable mass range, and perhaps varying other parameters such as matrix density and composition or sample size. The use of several standards helps confirm that  $CF(RL)$  and  $CF(AT)$  are being correctly determined and that Equation 6-2 is valid. If some nonlinearity is detected, the first concern should be to correct the problem(s), whether in equipment or in computation of  $CF(RL)$  or  $CF(AT)$ , rather than to add terms to the calibration equation. Modifying the calibration equation simply disguises the effects of poorly adjusted equipment, incorrect algorithms for  $CF(RL)$  and  $CF(AT)$ , equipment malfunction, or even outright ignorance of proper procedures and methods. After the equipment and the computational algorithms are as good as possible, if there is still some nonlinearity, then consideration can be given to modifying the calibration equation. Because such problems often result from a wide range of count rates, consider first two or more linear, two-parameter calibrations over more restricted mass ranges. Such adjustment of the calibration function should be required infrequently. The accuracy is more often limited by inhomogeneity or excessive particle size, and a single one-parameter linear calibration is nearly always sufficient.

The extent to which one may safely extrapolate a linear calibration beyond its data points depends on whether the extrapolation is toward lower or higher masses. At low concentrations of the assay isotope, the self-attenuation is usually dominated by the matrix, and  $CF(AT)$  changes very slowly over a wide range of concentration. Similarly, the count rates are low so that  $CF(RL)$  not only changes slowly but is small and accurately determined. As a result, one usually has high confidence when extrapolating down to the lowest detectable levels. As an example, consider the assay of  $^{235}\text{U}$  solutions by the 185.7-keV gamma ray. For reasonably sized samples (>25 mL), a concentration of  $\sim 10$  g/L  $^{235}\text{U}$  may well give a precision of  $\sim 0.5\%$  in  $\sim 1000$  s. A sample of 0.1 g/L  $^{235}\text{U}$  concentration has nearly the same  $CF(AT)$  and gives a precision of  $\sim 5\%$  in a 1000-s assay, which might well be acceptable. However, it would take  $\sim 100\,000$  s to count a 0.1-g/L  $^{235}\text{U}$  standard to 0.5% precision, which might well be required if it were included in the calibration data. A great deal of time can be wasted counting very low level standards.

The extrapolation to mass values higher than those in the standards must be approached more cautiously, especially if the highest mass standard is at a level where both  $CF(AT)$  and  $CF(RL)$  are changing rapidly or where the gross count rates are approaching the limits of the electronics to maintain adequate resolution and peak shape. The system performance at the higher masses and count rates should be confirmed with some source material even if no standard exists at the desired mass level. For example, if it has been confirmed that the system is able to accurately measure a transmission of 1% at a count rate of  $50\,000\text{ s}^{-1}$ , then there is reasonable confidence in assaying an unknown with 1% transmission at  $50\,000\text{ s}^{-1}$  even if the highest mass

---

standard has an  $\sim 2\%$  transmission and gives a gross rate of  $\sim 40\,000\text{ s}^{-1}$ . If the entire mass range gives only modest count rates and small and slowly varying values of CF(RL) and CF(AT), it is safer to extrapolate upward.

By way of final comment, the possession of an appropriate set of standards does not compensate for lack of knowledge of how to use them or for maladjusted or malfunctioning equipment, inappropriate assay geometries, incorrect expressions for the correction factors, or assay samples that do not adequately meet the requirements on uniformity and homogeneity. All the items are important factors in achieving accurate gamma-ray assays, and none can be safely neglected. When the pertinent factors are properly addressed, including proper and efficient use of calibration standards, gamma-ray NDA can provide economical, timely, and accurate assays for many materials.

## 6.8 GAMMA-RAY RATIO METHODS

Gamma-ray ratio methods are of some limited use in determining CF(AT). A detailed treatment of the many ratio techniques is beyond the scope of this book, but a short discussion can give the reader a feeling for some of the possibilities and limitations. The basic idea is to determine  $\mu_\ell$  and CF(AT) from the ratio of gamma-ray intensities at different energies. Consider a slab-shaped sample of thickness  $x$  containing an isotope that emits gamma rays at energies  $E_1$  and  $E_2$ ; assume that the unattenuated emission rates are equal. Using Equation 6-6, the peak area (A) ratio is

$$\frac{A_2}{A_1} = \frac{CF(E_1)}{CF(E_2)} = \frac{\mu_\ell(E_1)}{\mu_\ell(E_2)} \text{ for } \mu_\ell x \gg 1. \quad (6-20)$$

If the matrix composition or an "effective Z" is known or assumed, it may be possible to use the measured ratio of attenuation coefficients to determine the individual coefficients and evaluate CF(E). This is the idea behind all ratio methods, namely that different energy gamma rays are attenuated differently and may carry information about the attenuation properties of the material they pass through.

The gamma-ray ratio methods require the assumptions on uniformity and particle size discussed in Section 6.2.3 in order to give accurate results. If the assumptions are not met, the transmission-corrected methods give results that are usually low. Ratio methods give results that are generally greater than those from transmission methods, but may overcompensate depending on the size of the emitting particles.

Gamma-ray ratio methods require some additional knowledge of the sample. The required information varies with the procedure but often includes the sample density and the "effective" atomic number Z. The "effective" atomic number usually implies that the mass attenuation curve of the sample matches the curve for some single element. For multielement mixtures, especially those containing hydrogen, the curve may not closely match that of a single element.

In many cases, ratio methods can give a warning when the assumptions on uniformity and particle size are violated. Unfortunately, though the ratios can give a warning of potentially inaccurate assay situations, there is no way currently known whereby the ratio methods can consistently correct for the problems detected. A combination of transmission and ratio methods gives the most information about a given sample.

It is often assumed that the ratio methods are simpler to apply because they do not require the use of a transmission source. In practice it is doubtful that they are simpler because (a) the ratio methods require either the measurement or computation of the required "no attenuation" value of the ratio, (b) the ratio methods require some knowledge of the matrix composition, (c) in many applications the ratio method requires the net weight and volume of the sample, and (d) the ratio methods frequently require iterative procedures to arrive at the best result. Both transmission and ratio methods, for best results, will usually require a knowledge of the sample dimensions and its position relative to the detector.

## 6.9 ASSAY EXAMPLES

This chapter concludes with some topics useful to gamma-ray assays and a few actual measurement examples. The NRC-published *Handbook of Nuclear Safeguards Measurement Methods* (Ref. 13) gives the main design features and performance specifications for many gamma-ray assay systems.

### 6.9.1 Useful Gamma-ray Combinations for Assay, Transmission, and Reference Peaks

A sample of the material being assayed can sometimes be used as the transmission source, thus determining the transmission at exactly the required energy. Frequently, however, it is impossible to obtain such a source with sufficient intensity (uranium and plutonium are excellent at absorbing their own gamma rays). A number of considerations govern the choice of a transmission source for assaying a given isotope: the transmission gamma rays(s) should be close to the assay gamma-ray energy; the transmission energy should be lower than the assay energy so that the Compton continuum of the transmission gamma ray does not fall beneath the assay peak; the transmission gamma ray should not interfere with any gamma ray involved in the assay. Similar considerations apply to the choice of reference source for deadtime/pileup correction. Over the years many useful source combinations have been found and used. Table 6-2 gives some combinations which have been particularly useful.

### 6.9.2 Interpolation and Extrapolation of Transmission

Interpolating to an assay energy between two transmission peaks is preferable to extrapolating beyond one or more transmission peaks. Table 6-2 shows that the assay

---

Table 6-2. Useful source combinations

Isotope Assayed	Transmission Source	Correction Source
$^{238}\text{Pu}$ 766.4 keV	$^{137}\text{Cs}$ 661.6 keV	$^{133}\text{Ba}$ 356.3 keV
$^{239}\text{Pu}$ 413.7 keV	$^{75}\text{Se}$ 400.1 keV	$^{133}\text{Ba}$ 356.3 keV
$^{235}\text{U}$ 185.7 keV	$^{169}\text{Yb}$ 177.2, 198.0 keV	$^{57}\text{Co}$ 122.0 keV
$^{238}\text{U}$ 1000.1 keV	$^{54}\text{Mn}$ 834.8 keV	$^{137}\text{Cs}$ 661.6 keV
$^{237}\text{Np}$ 311.9 keV	$^{203}\text{Hg}$ 279.2 keV	$^{235}\text{U}$ 185.7 keV

of  $^{235}\text{U}$  by its 185.72-keV gamma ray with measured transmissions at 177.2 keV and 198.0 keV offers this advantageous situation. Assuming a linear relationship between transmission and energy, the transmission at any intermediate energy  $E$  is given by

$$T(E) = \left( \frac{E_2 - E}{E_2 - E_1} \right) T_1 + \left( \frac{E - E_1}{E_2 - E_1} \right) T_2 \quad (6-21)$$

If  $E = 185.7$ ,  $E_1 = 177.2$ , and  $E_2 = 198.0$ , then  $T(E) = 0.591(T_1) + 0.409(T_2)$ .

When the transmission gamma rays are close in energy (21 keV apart in this example), the linear interpolation is usually adequate, but if the transmission peaks are much farther apart, it may not be so. If three or more well-spaced gamma rays are emitted by the transmission source, it may be possible to fit the measured points to give accurate values of transmission for intermediate energies. If the gamma-ray attenuation of a given sample is dominated by a high- $Z$  element (uranium, plutonium, thorium, etc.), the mass attenuation coefficient of the sample is very close to a power law in energy:

$$\mu(E) = K E^{-\gamma} \quad (6-22)$$

where  $K$  and  $\gamma$  are constants. If this is true,  $\ln(-\ln T)$  vs  $\ln E$  is linear and interpolation over large energy ranges is feasible.

When only one transmission can be measured, correction to the assay energy is often possible based on approximate knowledge of the chemical composition of the sample. The applicable equation is

$$T_a = T_t^\alpha \quad (6-23)$$

where  $\alpha = \mu_a/\mu_t$

$\mu_a, \mu_t$  = mass attenuation coefficients at assay and transmission energies.

As an example, consider the assay of  $^{239}\text{Pu}$  (414 keV) contaminated incinerator ash using  $^{137}\text{Cs}$  (662 keV) as a transmission source. This mixture can be treated as two components, one having the attenuation properties of oxygen, and the other, those of plutonium. Table 6-3 illustrates the change in  $\alpha(\mu_a/\mu_t)$  with the plutonium weight fraction ( $F_{Pu}$ ). Because most incinerator ash is less than 10% plutonium by weight,  $\alpha = 1.27$  might be picked as an average value for the measurements.

Table 6-3. The variation in  $\mu(414)/\mu(662)$  with plutonium weight fraction

$F_{Pu}$	$\alpha = \mu(414)/\mu(662)$	
0	1.21	
0.1	1.33	
0.3	1.54	
0.5	1.71	
0.7	1.84	
0.9	1.95	
Mass Attenuation Coefficients (cm <sup>2</sup> /g)		
	414 keV	662 keV
$\mu_{Pu}$	0.26	0.13
$\mu_O$	0.093	0.077

### 6.9.3 Uranium-235 Assay in Far-Field Geometry

Table 6-4 gives the results of uncollimated, far-field assays for  $^{235}\text{U}$  in 13 standards of 4 distinct sample types. The germanium detector was located about 80 cm from the center of the samples. The reference source used for deadtime and pileup correction was  $^{241}\text{Am}$ . For standard types 1, 2, and 3, the correction factors for sample self-attenuation ( $CF_{186}$ ) were computed using  $\mu$  values derived from the measured gamma-ray transmissions ( $T_{186}$ ). The computational algorithms were similar to those discussed in Section 6.6.2. For the type 4 standards, which are uranium metal of accurately known mass and size, the correction factors were calculated from the simple far-field expression in Equation 6-6. Table 6-4 shows the corrected interaction rates per gram of  $^{235}\text{U}$  (response), which should be the same for all 13 standards. The response is normalized to the average of the three type 2 responses. The average of the 13 results is 0.999, the standard deviation is  $\sim 0.5\%$ , and the maximum deviation from the average is  $\sim 1.1\%$ . This represents excellent agreement, considering the wide range of size, shape, chemical composition, and uranium content, especially noting that the correction factors range from 1.26 to 3.30.

Table 6-4. Calibration standard intercomparison

Standard	Type 1				Type 2			Type 3			Type 4		
Container	polypropylene bottle							3-dram vial			thin plastic bag		
Size/shape	8.26 cm i.d. × 17 cm high							14.7 mm i.d. × 5 cm high			disk 5.08 cm diam × 0.25 to 0.50 mm thick		
Composition	U <sub>3</sub> O <sub>8</sub> & graphite				solution U & HNO <sub>3</sub>			solution U & HNO or HCL			U metal		
<sup>235</sup> U (%)	92.83				10.08			93.12			93.15		
Uranium (g)	200.0	100.0	50.0	10.00	155.8	103.7	52.0	4.246	2.546	0.848	21.49	9.579	9.058
<sup>235</sup> U (g)	185.7	92.8	46.4	9.28	15.70	10.45	5.24	3.956	2.371	0.790	20.02	8.92	8.44
T <sub>186</sub>	0.022	0.091	0.184	0.335	0.033	0.064	0.123	0.249	0.377	0.588	0.210	0.499	0.518
CF <sub>186</sub>	3.30	2.32	1.88	1.54	2.994	2.552	2.132	1.729	1.493	1.263	1.976	1.388	1.365
Response (s-g <sup>235</sup> U) <sup>-1</sup>	5.104	5.038	5.042	5.096	5.084	5.116	5.090	5.104	5.110	5.104	5.101	5.074	5.074
Normalized response	1.002	0.989	0.989	1.000	0.998	1.004	0.999	1.002	1.003	1.002	1.001	0.996	0.996

The results show that any of the four sets could serve as practical standards for far-field gamma-ray assay of any of the other sets. Some gamma-ray procedures (for example, near-field segmented scanning) are not as insensitive to size and shape as the far-field procedures. Still, a relatively small set of physical standards can usually calibrate most passive gamma-ray assay systems.

#### 6.9.4 Plutonium-239 Solution Assay in Near-Field Geometry

The assay geometry indicated in Figure 6.16 is used for the near-field assay of  $^{239}\text{Pu}$  in solution. The sample bottle is a right-circular cylinder with a bottom area of  $10\text{ cm}^2$  and depth of 4.0 cm. The maximum sample volume is 40 mL; however, typical sample volumes are only 25 mL. The sample is only about 5 cm from the detector end cap and the distance to the effective interaction depth is 7 or 8 cm. This is a distinctly near-field situation that creates increased difficulties in correctly

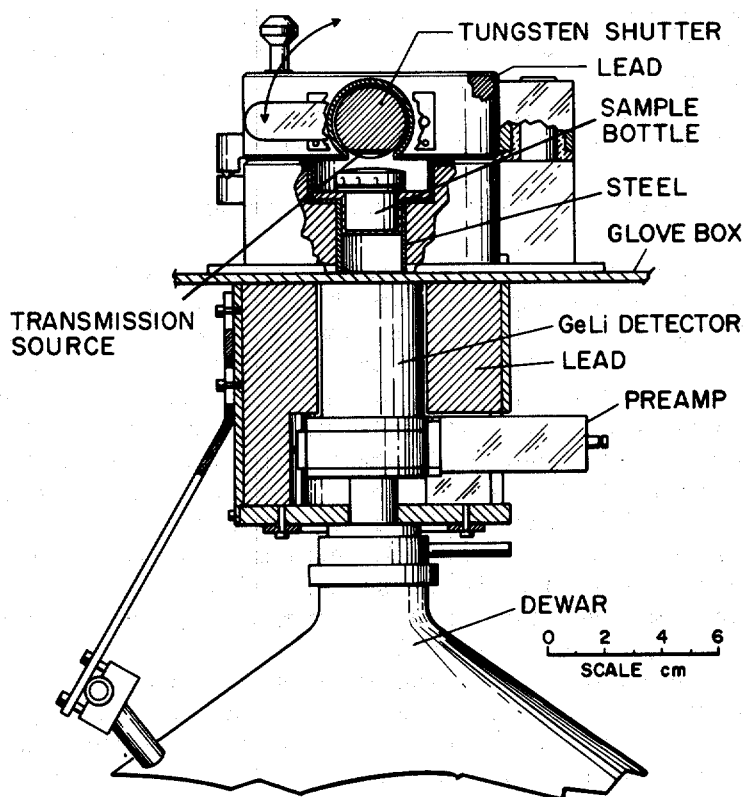


Fig. 6.16 Cutaway drawing showing arrangement of the detector, sample, and shielding used for the near-field assay of  $^{239}\text{Pu}$  in solution.

computing the CF(AT). In principle, one would like to increase the sample-to-detector distance in order to simplify the computations. Unfortunately, that would reduce the count rates to where the required assay times would be excessively long.

The 88.0-keV gamma ray of  $^{109}\text{Cd}$  is used as the reference for deadtime/pileup corrections. The reference source is fastened firmly to the detector end cap. To avoid interpolation or extrapolation, a plutonium metal disk is used as the transmission source so it is necessary to make separate sample-alone and sample-with-source runs and subtract to obtain the transmissions. For lower plutonium concentrations, the more intense 129.3-keV gamma ray gives more precise transmission values and a more precise overall assay than does the 413.7-keV gamma ray. At higher concentrations, the 413.7-keV gamma ray with its higher penetrability has both better signal and transmission and gives a more precise assay than does the 129.3-keV gamma ray. The weighted average of the 129.3- and 413.7-keV-based assays is used for the final assay, giving an overall measurement precision that is quite flat over a wide range of concentration.

This assay system uses the one-dimensional model for CF(AT) described in Section 6.6.2. The sample-to-detector distance is an adjustable parameter to flatten the plot of total corrected rate vs concentration. When properly adjusted and calibrated, this system measures  $^{239}\text{Pu}$  in plutonium solutions with a bias of <1% for concentrations from 1 to 400 g Pu/L. Using 1000-s counts for both the sample-only and sample-with-transmission source runs, the precision is <1.0% for all concentrations of >1 g Pu/L.

### 6.9.5 Transmission-Corrected Segmented Scanning

In Section 6.6.4, segmented scanning was given as an example of an assay procedure in which a relatively simple three-dimensional model could be used to calculate CF(AT). This section concludes with some discussion of the reasons for using such a procedure and of some actual geometrical configurations and source combinations.

In the process of filling scrap and waste containers, vertical variations frequently occur in the volume densities of both source and matrix materials. Radial inhomogeneities are often less pronounced, and their effects can be substantially reduced by sample rotation. The different layers may substantially meet the requirements on homogeneity even though large differences exist between layers. In such cases the container may be assayed as a vertical stack of overlapping segments. The advantages of the segmented scanning procedure are gained at the loss of some degree of sensitivity; hence a system employing segmented scanning would probably not be used on samples containing <1 g of  $^{239}\text{Pu}$  or  $^{235}\text{U}$ .

Figure 6.17 shows the spatial relationships of detector, collimator, assay sample, transmission source, and reference source for a system tailored to the assay of  $^{239}\text{Pu}$  in cylindrical containers <20 cm in diameter. It also gives approximate values for the intensities of the transmission and reference sources. Figure 6.18 shows a photograph of a segmented gamma scanner (SGS).

---



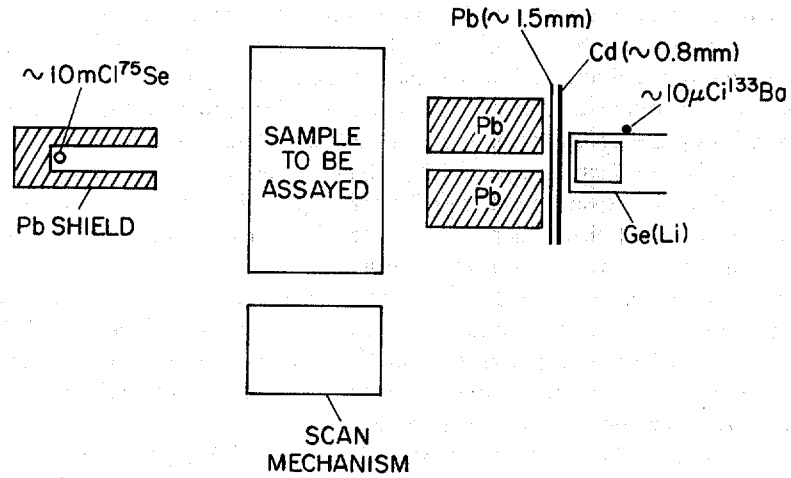


**Fig. 6.17** General arrangements for segmented, transmission-corrected, gamma-ray assay. The specific situation shown is tailored to the assay of  $^{239}\text{Pu}$  in cylindrical containers.

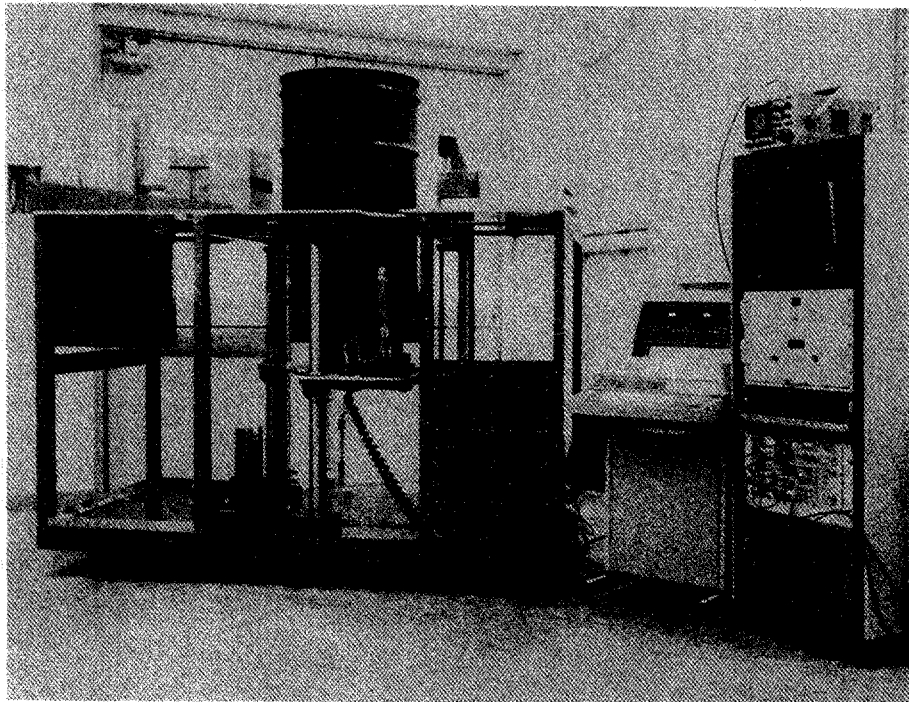


**Fig. 6.18** SGS system showing scan table for 55-gal. drums.

The sample container is positioned as close as possible to the collimator to maximize count rates and give the best segment resolution. The segment overlap is determined by the sample size, collimator dimensions, and the relative positions of the segments. In Figure 6.17, a collimator 1.25 cm high and 10 cm deep provides a reasonable trade-off in sensitivity and spatial resolution. For 30- and 55-gal. drums, a collimation 5 cm high and 20 cm deep is a reasonable choice. The spatial resolution cannot be as sharp in the latter case, but it is sufficient to provide useful information on the uniformity of material distribution. The choice of collimator material is usually lead. If space is a consideration, a tungsten alloy may be used.

To maximize count rates, the detector is as close as possible to the collimator. For the plutonium measurement, a filter of lead ( $\sim 1.5$  mm) and cadmium ( $\sim 0.8$  mm) reduces the rate of low-energy events from  $^{241}\text{Am}$  and the x rays of both plutonium and lead. For  $^{235}\text{U}$  assay, the cadmium alone should suffice, because there is not the 60-keV  $^{241}\text{Am}$  flux found in plutonium materials.

For  $^{239}\text{Pu}$  assay,  $^{75}\text{Se}$  is the transmission source and  $^{133}\text{Ba}$  is the reference source. About 10 mCi of  $^{75}\text{Se}$  provides usable intensity for at least 1 yr in spite of the relatively short 120-day half-life. Sources of this strength must be encased in a collimator shield to avoid undue personnel exposure. The 356.0-keV gamma ray of  $^{133}\text{Ba}$  provides the reference; it can also be used for spectrum stabilization because it is always present in the acquired spectrum. The 10.4-yr half-life is convenient; a single source usually lasts the useful life of a germanium detector. A source of  $\sim 10$   $\mu\text{Ci}$  may be positioned anywhere on the front or side of the detector end cap; however, a slightly better peak shape results when the source is mounted on the front of the end cap along the crystal axis.

Segmented scans may be accomplished in several ways, described as discrete or continuous scans. In a continuous scan, the rotating sample moves past the collimator at a constant speed. The count time is often chosen as the time required for the container to move the height of the collimator. In a discrete scan, the sample is positioned vertically, counted, repositioned, counted again, etc. This mode of operation avoids detector microphonics caused by vibration in the vertical drive system. In practice, a segment spacing equal to one-half of the collimator height works well and might be recommended as a "rule of thumb." The continuous mode probably gives a somewhat better value for the average transmission within a segment. The discrete scan is usually easier to achieve. It also lends itself to two-pass assays in which the container is counted once with the transmission source exposed and once with it shuttered off. The two-pass scheme is useful when the utmost sensitivity and accuracy is desired, and is particularly useful when  $^{169}\text{Yb}$  is used as a transmission source in  $^{235}\text{U}$  assays. Other variations in the application of the segmented scanning procedure are possible and are described in Refs. 14 and 15.

**REFERENCES**

1. *American National Standard Guide to Calibrating Nondestructive Assay Systems*, ANSI N15.20-1975 (American National Standards Institute, New York, 1975).
  2. J. L. Parker, "The Use of Calibration Standards and Correction for Sample Self-Attenuation in Gamma-Ray Nondestructive Assay," Los Alamos National Laboratory report LA-10045 (August 1984).
  3. J. H. Hubbell, "Photon Cross Sections, Attenuation Coefficients, and Energy Absorption Coefficients from 10 keV to 100 GeV," National Bureau of Standards report NSRDS-NBS 29 (August 1969).
  4. J. P. Francois, "On the Calculation of the Self-Absorption in Spherical Radioactive Sources," *Nuclear Instruments and Methods* 117, 153-156 (1974).
  5. J. L. Parker, "A Correction for Gamma-Ray Self-Attenuation in Regular Heterogeneous Materials," Los Alamos National Laboratory report LA-8987-MS (September 1981).
  6. J. L. Parker and T. D. Reilly, "Bulk Sample Self-Attenuation Correction by Transmission Measurement," Proc. ERDA X- and Gamma-Ray Symposium, Ann Arbor, Michigan, May 19-21, 1976 (Conf. 760539).
  7. W. H. McMaster, N. Kerr Del Grande, J. H. Mallett, and J. H. Hubbell, "Compilation of X-Ray Cross Sections," Lawrence Radiation Laboratory report UCRL-50174, Sec. II, Rev. 1 (1969).
  8. J. E. Cline, "A Technique of Gamma-Ray Detector Absolute Efficiency Calibration for Extended Sources," Proc. American Nuclear Society Topical Conference on Computers in Activation Analysis and Gamma Ray Spectroscopy, Mayaguez, Puerto Rico (1978), pp. 185-196 (Conf. 780421).
  9. "Self-Shielding Correction for Photon Irradiation of Slab and Cylindrical Samples," Gulf General Atomic, Inc., Progress Report GA-9614 (July 1, 1968-June 30, 1969).
  10. *Handbook of Mathematical Functions With Formulas, Graphs, and Mathematical Tables*, Milton Abramowitz and Irene A. Stegun, Eds., National Bureau of Standards, Applied Mathematics Series 55 (1970).
  11. Yardley Beers, *Introduction to the Theory of Error* (Addison-Wesley Publishing Co., Inc., Reading, Massachusetts, 1962).
-

12. Philip R. Bevington, *Data Reduction and Error Analysis for the Physical Sciences* (McGraw-Hill Book Company, New York, 1969).
  13. *Handbook of Nuclear Safeguards Measurement Methods*, Donald R. Rogers, Ed., NUREG/CR-2078, MLM-2855 (US Nuclear Regulatory Commission, Washington, DC, 1983).
  14. E. R. Martin, D. F. Jones, and J. L. Parker, "Gamma-Ray Measurements with the Segmented Gamma Scan," Los Alamos Scientific Laboratory report LA-7059-M (December 1977).
  15. American Society For Testing and Materials, "Standard Test Method for Nondestructive Assay of Special Nuclear Material in Low-Density Scrap and Waste by Segmented Passive Gamma-Ray Scanning," Vol. 12.01, C853-82, 1989, p. 366, ASTM, Philadelphia.
-